J. Earth Syst. Sci. (2022)131 18
https://doi.org/10.1007/s12040-021-01752-6

Tectonic instability of the petroliferous upper Assam valley (NE India): A geomorphic approach

Manash Pratim Gogoi[1], Bikash Gogoi[2] and Soumyajit Mukherjee[3,*]

[1]*Department of Geology, Sibsagar College, Joysagar, Sivasagar, Assam 785 665, India.*
[2]*Department of Geological Sciences, Gauhati University, Guwahati, Assam 781 014, India.*
[3]*Department of Earth Sciences, Indian Institute of Technology Bombay, Powai, Mumbai, Maharashtra 400 076, India.*
**Corresponding author. e-mail: soumyajitm@gmail.com smukherjee@iitb.ac.in*

MS received 4 January 2021; revised 28 June 2021; accepted 31 August 2021

Tectonic (in)stability of terrains is of major concern in financial investment for hydrocarbon exploration from such terrains. Morphometric studies of a river can explain neotectonics of the terrain. This study presents the southeast (SE) frontier of the Brahmaputra river valley of the upper part of the state of Assam, northeast India, where geomorphic changes are observed through remote sensing studies. Two primary geomorphic observations of the study are: (1) formation of palaeostream at the valley due to cut-off of headwater discharge due to the activation of frontal thrust (Naga thrust) along the SE boundary of the valley and the Naga Hills (Assam–Arakan fold-thrust belt), and (2) shifting of confluence points Lohit river (tributary of the Brahmaputra river) causing avulsion and formation of a river island (Dibru Saikhowa). The first event is related to the recent tectonic activities, i.e., uplift of a fault-propagation fold (Digboi anticline). The later event of migration of the Lohit river might be associated with tilting of the SE side of the basin due to activities along the blind thrust systems of the Himalayan foot-hills and the basement high over the last 25 years. This gradually elongated its drainage basins. The southern propagation of the frontal thrust systems of Arunachal Himalaya and Mishmi hills has already shifted the course of the Lohit river towards the south leading to significant changes in geomorphology over the last few decades. N–S-oriented compressional stress axis apparently indicates possible movements along the fault systems bounding the inter-drainage basin facilitating the fluvio-morphometric changes.

Keywords. Morphometry; neotectonics; relief; remote sensing; physical geology; geomorphology.

Abbreviations

BDB	Burhi Dihing basin
DB	Dibru basin
DT	Disang thrust
IDB	Intra-drainage basin
MBT	Main Boundary Thrust
MFT	Main Frontal Thrust
MT	Mishmi thrust
NDB	Noa Dihing basin
NT	Naga thrust
SH_{max}	Orientation of maximum horizontal stress
mag	Magnitude scales: local magnitude or richter magnitude
NF	Normal Faulting
SS	Strike-slip
TF	Thrust Faulting
U	Unknown

Published online: 10 January 2022

1. Introduction

Rivers are nature's one of the most adaptive, powerful and spontaneous forces, which slowly yet continuously shape the landforms over the Earth's surface. They are the outcomes of complex interactions between the precipitations with the terrain configuration. Morphologies of the rivers are sensitive to tectonics (Vita-Finzi 2012; Whittaker 2012). Geomorphological analyses have proved vital in petroleum geosciences studies (e.g., Conybeare 1976; Babu 1994). This is because geomorphology such as drainage pattern can be fault or basement structure-controlled. Neotectonic stress regime can work with them and produce surface morphology (e.g., Mazumder *et al.* 2012).

The Brahmaputra (also known as *Mohabahu*, *Luit* and *Borluit* in Assam) river is one of the largest braided rivers of the Indian subcontinent that flows through the state of Assam, northeast (NE) India. The Assam valley is marked by the foothills of the Himalayan mountain belt towards the north, Mishmi Hills of Arunachal Pradesh towards the east and the Naga Hills of the Assam–Arakan fold-thrust belt, also called the belt of Schuppen (Ghosh *et al.* 2010; Aier *et al.* 2011; Kent *et al.* 2002) towards the south. The Brahmaputra flows in the middle of this valley from the NE towards the southwest (SW). Towards the upper part of Assam, three major tributaries, viz., Dihang (or Siang), Dibang and Lohit confluence form the mighty Brahmaputra river near Dibrugarh (figures 1 and 3). Other sub-streams originating from the Himalaya, Mishmi and the Naga hills have created a huge network of drainage for the Brahmaputra. Dihang (or Siang in Arunachal Pradesh) on the upstream beyond India is known as the Yarlung–Tsangpo river and originates from the Kubi, Chemayungdung and Angshi glaciers (Dwivedi 2016). Qiao and Yi (2017) reported that the Ganglung, the Gangri, the Rachama and the Kubi Gangri glaciers are the sources of the Yarlung–Tsangpo river from an ∼6256 to 6859 m elevation. Tributaries of the Brahmaputra can be divided into two categories, viz., (1) those originating from the Himalaya and Mishmi hills, and (2) few originating from the Naga Hills and Meghalaya located in the southern side of the valley. Dihang (/Siang), Dibang, Jiadhal, Kumotia, Subansiri, Dikrong, Jia Bhareli (/Kameng) and Puthimari are included in the first group. Rivers such as Lohit, Nao Dihing, Dibru, Burhi Dihing, Disang, Dikhow, Jhanji, Dhansiri, Sonai, Kopili come under the second group. However, Lohit originates from the Mishmi hills. Preordained by this huge network of drainage, this part of NE India has promising significance for environmental geoscientific studies (Goswami 1984) and prospects of hydropower generation (Das 2014).

The drainage basin of river Brahmaputra has a dynamic network of streams where the channel shifts repeatedly (Gogoi and Goswami 2014) and changes its shape (Goswami and Acharjee 2016) leading to river capturing (Prasad 2014), avulsion (Chopra 1980; Borgohain *et al.* 2016; Lahiri and Sinha 2012; Sah and Das 2018), development of paleo-streams (Saikia and Amin 2016) and the formation of abandoned channel segments (Dutta and Konwar 2013). These modifications are often associated with the change in the headwater sources (Stella *et al.* 2011; Toonen *et al.* 2012), neotectonics (Malik and Mohanty 2007; Zámolyi *et al.* 2010; Whitney and Hengesh 2015) or due to climatic changes (Verhoog 1987). Several fluvial changes in the drainage system of river Brahmaputra around Majuli district have been reported, viz., superimposition of bank lines, bank line shifting and bank line erosion (Sarma and Phukan 2003).

The eastern side of the Noa Dihing river is bound by a NW–SE trending Manabum anticline (figures 1 and 2) produced due to slip-induced drag (Mukherjee 2014) of the Mishmi thrust (MT) (Ghosh *et al.* 2010). The river Burhi Dihing parallels the NE–SW trending Naga hills (Schuppen belt) and later crosses the Naga thrust (NT) through the Digboi anticline (figure 2) (Kent *et al.* 2002) near Namsang Tea Estate, after crossing the Margherita, Tinsukia district, Assam. The belt of Schuppen located to the SE of the valley is a regional structure resulting from complex imbrications of thrust and duplexes of several thrust systems, viz., the NT, the Disang thrust (DT) (figure 1) and the subsidiary thrust sub-splays (Angelier and Baruah 2009; Alam *et al.* 2019).

The tectonic set up of the Assam valley, a result of the Himalaya–Tibet and Indo-Burmese collisions (Nandy 2001; Raoof *et al.* 2017; Alam *et al.* 2019) is demarcated by the Arunachal Himalaya, Mishmi Hills (eastern Himalayan syntaxis, Yin 2006; Alam *et al.* 2019) and the Assam–Arakan fold-thrust belt (figure 1). It is a seismically active region as several earthquakes have been reported. The USGS data (https://earthquake.usgs.gov/earthquakes) reveal that between 12 December 1908 and 22 November 2020, a total of 167

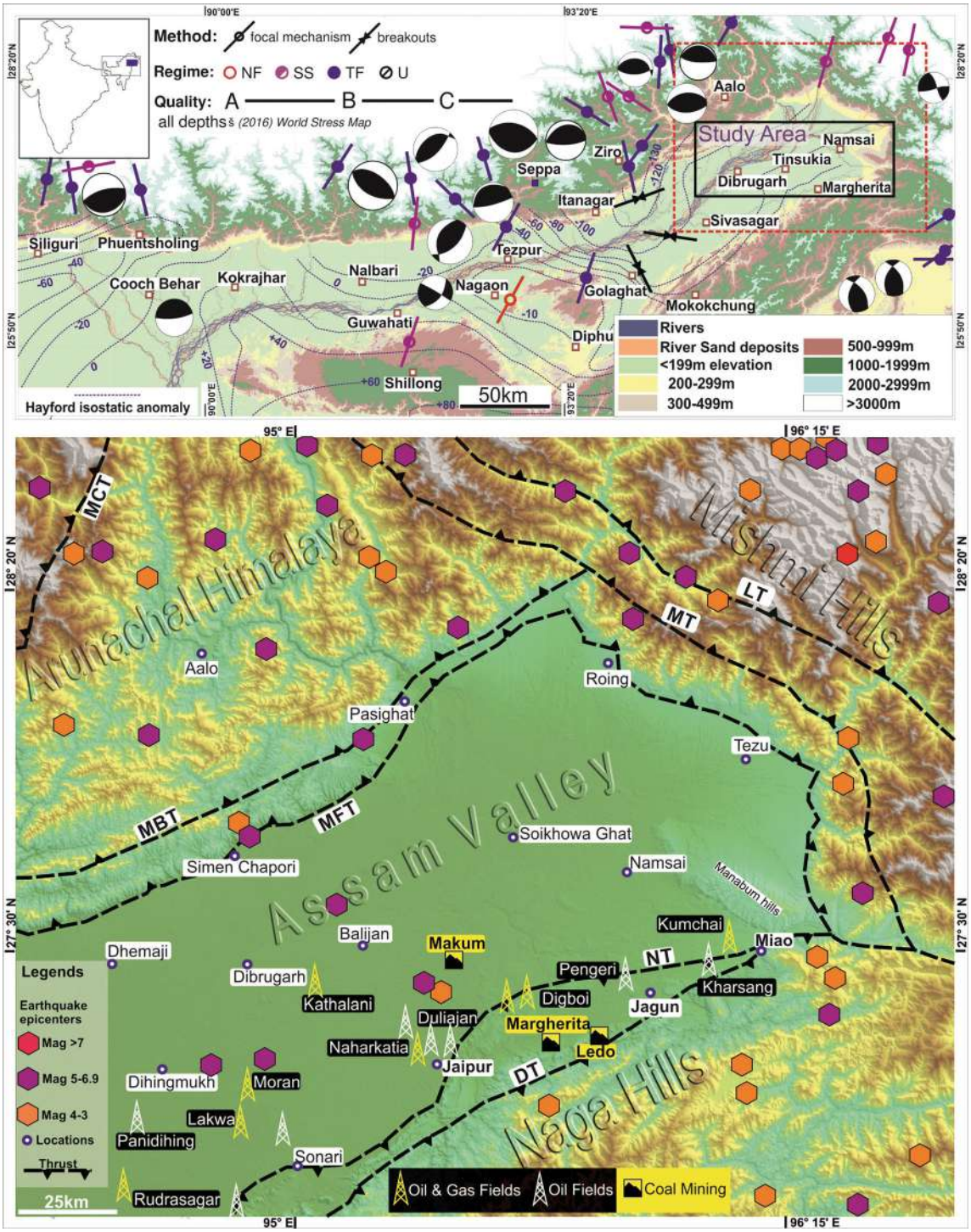

Figure 1. **Top**: CartoDEM showing physiography of the NE India with rivers and sand deposits traced from 2020 Landsat OLI 8 data using pixel analyses, along with the stress regimes from the World Stress Map database (created from CASMO, Heidbach *et al.* 2016; also see Zoback 1992), focal mechanism (after Dasgupta *et al.* 2000; Verma 2002) and Hayford isostatic anomalies (after Verma and Mukhopadhyay 1977) and the study area. From the World Stress Map (WSM) data, orientation of maximum horizontal stress (SH_{max}) along TF (thrust faulting) shows ENE–WSW near Assam–Arakan folded belt, NNE–SSW near Mikir Massif (Golaghat), NE–SW to NNW–SSE, NW–SE to NNW–SSE, NNE–SSW to NE–SW near orientation at Arunachal Himalaya. SH_{max} are oriented along SS (strike−slip) faults in NNE–SSW to NW–SE at Mishmi Hills and Arunachal Himalaya. Near the western edge of Mikir Massif, SH_{max} is oriented along NF (normal faulting) in NE–SW direction. **Bottom**: CartoDEM image of study area of the upper part of Assam valley, surrounded by Himalayan foothills marked by MFT and MBT on north, Mishmi hills marked by MT on east and Naga–Patkai range marked by NT and DT. Two anticlinal structures are present at Digboi and Manabum areas. The map also shows earthquakes that occurred in the area between the years 1908 and 2020. (Faults are after Das Gupta and Biswas 2000).

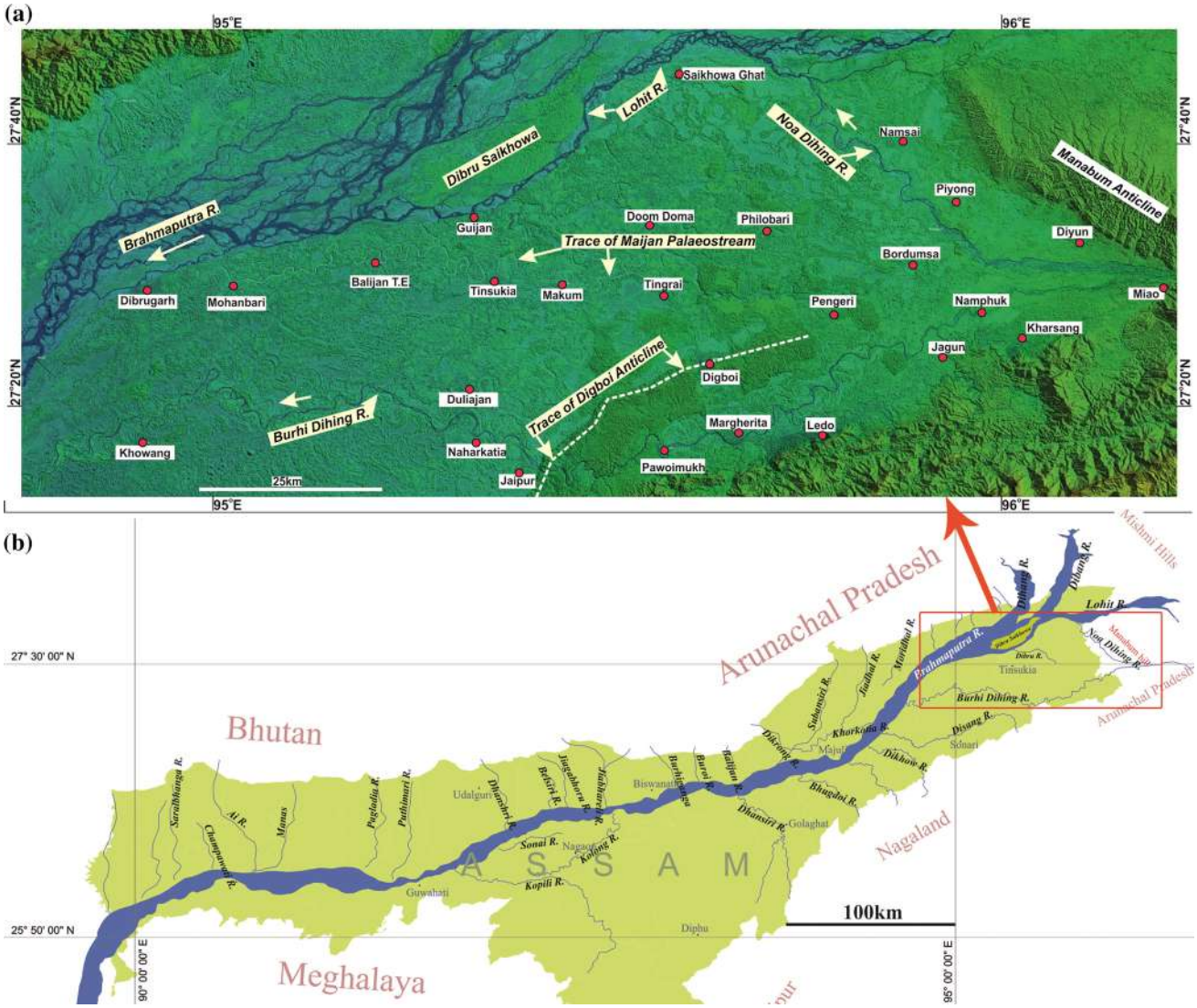

Figure 2. CartoDEM images (**a**) showing the trace of Maijan Palaeostream, Digboi Anticline, Manabum Anticline, Dibru Saikhowa, Lohit, Noa–Dihing and Burhi–Dihing river and (**b**) drainage of Brahmaputra and its major tributaries through the state of Assam.

earthquakes of >2.5 magnitude took place in the region (figure 1; depth and magnitude information in figure 3a and b). The maximum compressive stress ($S_{H\max}$) vectors obtained from the world stress map (Heidbach *et al.* 2016) gives the idea of the plate movement in this portion (also see Yadav and Tiwari 2018). NNW–SSE to NE–SW oriented $S_{H\max}$ vectors in the study area (figure 1) suggests N–S compression driving the frontal thrust sub-splay systems of the Mishmi and the Assam–Arakan fold-thrust belt.

The geology of the Brahmaputra basin has been briefly reviewed in Talukdar *et al.* (2004). This part of the upper Assam valley is important for oil and coal production. Several oilfields and coal mines (figure 1) are located (Kent and Dasgupta 2004). This region is bounded by the foothill ranges of the Himalaya and the Assam–Arakan fold-thrust belt. N and NE limits of the valley are marked by the Main Frontal Thrust (MFT) and the Mishmi Thrust (MT) (figure 1). The southern part of the valley is tectonically marked by the northward propagation of NT below the Digboi anticline (Kent *et al.* 2002), which is the frontal extension of the Naga-Patkai hills range. The Digboi oil field is located in the hanging wall of the NT system (Mathur and Evans 1964). The Paleogene and Neogene sediments over the Precambrian basement rocks, marked by several Oligocene, Miocene and Pliocene unconformities are recorded in this part of the Brahmaputra valley (Mathur and Evans 1964; Handique *et al.* 1989; Mathur *et al.*

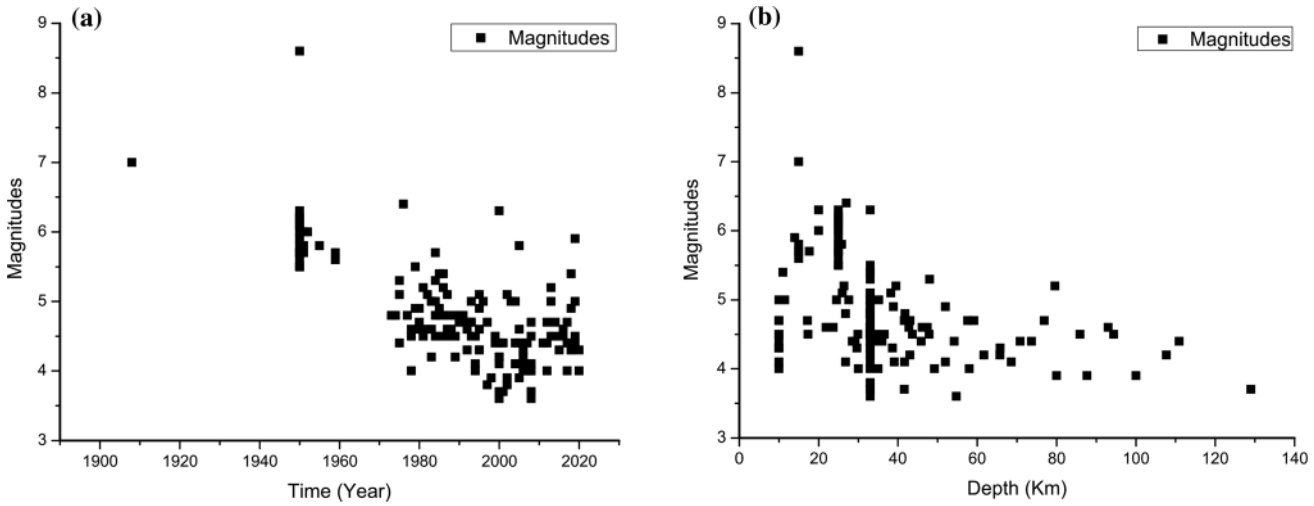

Figure 3. Scattered plot showing (**a**) earthquakes occurred between 1908 and 2020 in the area shown in figure 1 (bottom), out of these 168 earthquakes, 2 are above 7 mag, 60 between 5 and 6.9 mag and the remaining 105 are between 3.6 and 4.9 magnitude, and (**b**) between 1908 and 2020, several earthquakes ranging from 5 to 8 magnitude occurred in the year 1950, and most of the other earthquakes had occurred in the last 40 years. Nine out of 167 earthquakes are from depth zone 80–129 km, 15 are from depth 50–79.6 km, 28 from 35 to 49.2 km and the rest 115 from depth 10–34.7 km.

2001). Similarly, Tertiary rocks of equivalent age overlying the Precambrian rocks have been recorded in the Schuppen belt (Evans 1932; Ranga Rao 1983; Deshpande *et al.* 1993).

Between Margherita and Jaipur (figure 2), lies the Digboi doubly plunging anticlinal structure, which resulted from the NT (Kent *et al.* 2002), the river Burhi Dihing flows along the trend of the foredeep basin created on the SE back-limb of the structure. The tectonic framework substantially controls the drainage networks in the upper part of the Brahmaputra valley. Lahiri and Sinha (2012) reported from seismic survey that the development of basement 'highs', channel incorporation to form Majuli river island and abandonment by the river Brahmaputra is attributed to morpho-tectonic evolution of fluvial dynamics.

Sahoo and Gogoi (2010a) presented a stratigraphy of the upper Assam basin. Correlating geophysical data with surface observations, they concluded that during the Eocene, dominantly an estuary condition persisted with typical progradational, aggradational and transgressive regressive stacking patterns of sediments. Sahoo and Gogoi (2010b) summarised the evolution of this basin as '*…a unique polycyclic basin that involves a shift from Paleocene–Oligocene passive margin setting to Miocene foreland phase followed by an intermountain basin*'. Geophysical studies by these authors pointed out the presence of NE and ENE-trending blind normal faults that were more active during Oligo−Miocene time. Deb *et al.* (2012) through paleogeographic studies pointed out the areas of high prospect for future exploration from the upper Assam basin in areas such as Khagorijan (near Sepon, Sivasagar district) and Baghjan (near Doom Dooma, Tinsukia district). The terrain analyses with remote sensing by Kunte (1988) of Naga foothills and Mikir massif identified several geomorphic anomalies in the Naga piedmont along the NT systems, which bears prospects of hydrocarbon generation and entrapment. Singh *et al.* (2012) produced quantitative models to explain the impact of the Schuppen belt on the petroleum systems in the north Assam shelf in crucial aspects such as maturity, generation of petroleum in both the shelf and the sub-thrust area.

In Dibrugarh district, several palaeostreams have been identified in satellite imageries. This study aims to delineate and to find out the cause of the formation of one of the palaeostream called Maijan. This study also documents the changes in the course of the Lohit river located at the eastern frontiers of the Brahmaputra valley near Dibru Saikhowa National Park area and to find out the possibility of involvement of neotectonic activities along the MT and NT systems or at the basement arch (Das Gupta and Biswas 2000; Pahari *et al.* 2008; Borgohain *et al.* 2017). The study is focused to assess the loss of landmass brought by fluvio-morphometric changes and to determine the cause of formation of palaeo-streams.

The petroliferous upper Assam basin has been considered as a category III inter-orogenic foreland

basin. Various geoscientific techniques were applied in this basin by the oil industry (Biswas *et al.* 1993). Thus far, geomorphological approach to study tectonic instability remains to be explored. This paper fulfills the gap.

2. Study area

The study area (27°47′15″–27°6′10″N; 96°26′15″–94°37′3″E) is located in the upper Brahmaputra valley. This area is circumscribed by rivers and hence it is an inter-drainage basin (IDB) bounded by the Nao Dihing river at the NE, Burhi Dihing river at SE and SW, and Lohit–Brahmaputra at N–NW (figure 4). The area of this IDB is ∼1450 km^2 (figure 4). Noa Dihing river confluences with Lohit river near Saikhowa ghat, and Burhi Dihing river discharges into the Brahmaputra at Dihingmukh. Noa Dihiang is also known as Diyun river upstream of Miao. After passing Miao near Maithong, Burhi Dihing attains its separate entity from Diyum. Subsequent connections of sub-streams with these rivers increase their sizes and magnitudes.

3. Methodology

We used: (1) Landsat 8 OLI, 4–5 TM and 1–5 MSS from the United States Geological Survey (USGS) – Representational State Transfer (REST) Landsat product archive accessed through EarthExplorer (https://earthexplorer.usgs.gov/), (2) IRS-P6 LISS-III, (3) AWiFS 56 m spatial resolution, (4) Carto DEM made available by the National Remote Sensing Centre (NRSC-ISRO), (5) 1955 US Army Toposheet from University of Texas Library and (6) Google Earth Pro Landsat imageries. These inputs were processed in GIS applications, viz., QGIS 3.14 (π edition), Global Mapper v.11 and Google Earth Pro to obtain maps and analytical data as in figure 5.

Band-2 (blue), band-3 (green) and band-4 (red) of the Landsat data are used to produce the false colour composites. To conduct the morphometric analyses, the selected morphometric parameters have been categorised: (1) relief category: consisting of basin relief (H), relief ratio (Rh) and relative relief (Rhp); (2) aerial category: consists of form factor (Rf), circularity index (Rc) and elongation ratio (Re) and (3) tectonic category: consists of parameters – hypsometric integral (Hi), mountain-front sinuosity (Smf), asymmetry factor (AF) and transverse topographic symmetry (T) were carried out in the composite basin of Noa Dihing, Burhi Dihing and the Dibru rivers. Table 1 defines these parameters mathematically.

Basin relief (H) is the difference between the highest and lowest elevations of the basin (Strahler 1952). It gives the overall relief of the basin. Higher the value of H indicates high surface runoff. The relief ratio (Rh) (Schumm 1956) is the ratio between basin relief and basin length (Lb), which resembles the expression of the slope, i.e., the ratio

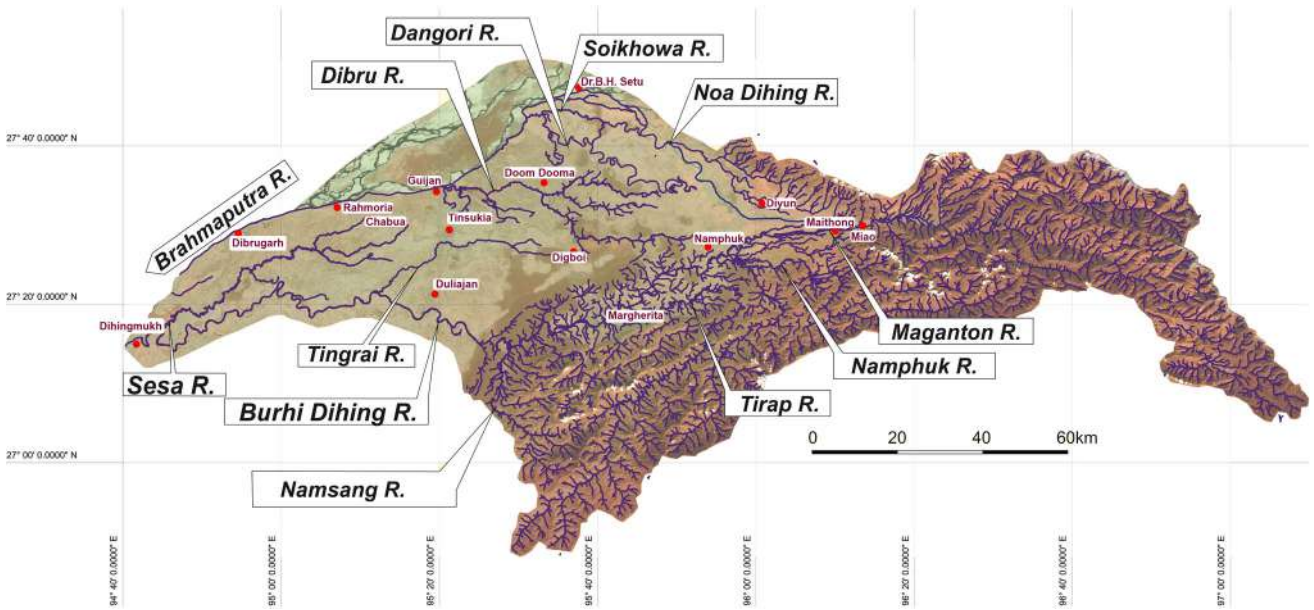

Figure 4. AWiFS imagery of the study area showing drainage systems of IDB Noa–Dihing, Burhi–Dihing, Lohit and Brahmaputra rivers.

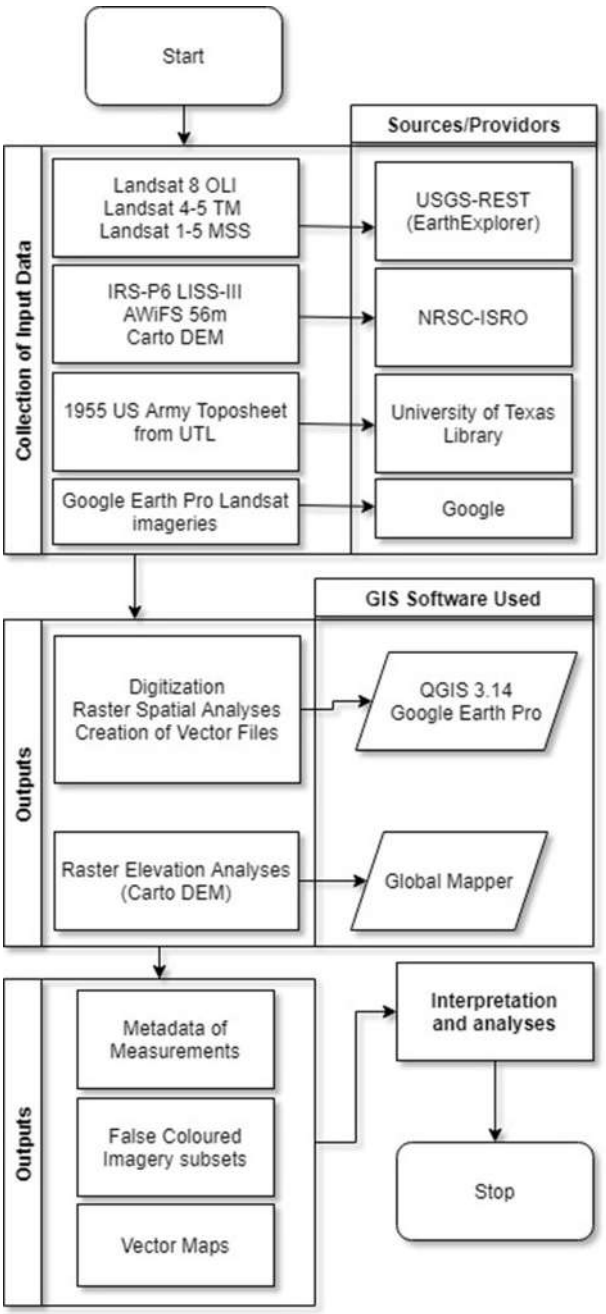

Figure 5. Flow chart depicting work-flow of the GIS-based studies.

between vertical and horizontal change. Therefore, *Rh* gives the idea of the overall slope of the basin. The value of *Rh* indicates the rate of discharge and eventually the rate of erosion by runoff. Relative relief (*Rhp*) is a ratio between basin relief and perimeter (Melton 1957), is an expression of overall steepness of a basin to the outlet.

The aerial parameter, the form factor (*Rf*) (Horton 1932) is the ratio between the actual basin area (*A*) to the area of an imaginary basin whose length is equivalent to the actual basin length (i.e., square of the basin length, L^2). A smaller value indicates an elongated basin. The circularity ratio (*Rc*) (Miller 1953) is a ratio between the basin area to the area of a circle with circumference similar to that of the perimeter of the basin. The value of *Rc* closer to 1 indicates circular basin. The elongation ratio (*Re*) (Schumm 1956) is the ratio between the diameter of an imaginary circle with an area similar to the basin – the length of the basin. It can indicate the shape of the basin – circular, oval or elongated.

The hypsometric integral (*Hi*) (Strahler 1952; Bull and McFadden 1977) is the ratio between two factors, i.e., the difference of the lowest elevation from the mean and maximum elevation, as presented in table 1. It determines the nature of evolution of basin topography with respect to the catchment area. The mountain front sinuosity (*Smf*) (Bull and McFadden 1977) is the ratio between lengths along the mountain front to the linear length. A high value of the *Smf* indicates an active mountain front. The asymmetry factor (*AF*) (Cox 1994; Keller and Pinter 2002) is the ratio of the right-hand side of the downstream basin area with the basin area, which is an expression of the degree of symmetry of the basin shape and affected by tectonic tilting. The transverse topographic symmetry (*T*) (Cox 1994) is the ratio between the distance from the active meander-belt midline to the basin midline (*Da*) and the distance from the basin divide to the basin midline (*Da*). It can be used to determine tectonic control over the basin (Cox 1994).

A comparison between the Landsat 1–5 MSS, 4–5 TM and 8 OLI images of different time intervals (table 5) along with the 1955 US army topo-sheet has been done using GIS software to estimate the changes that occurred within IDB consists of Burhi Dihing, Dibru river and Noa Dihing river basins as well as around the Dibru Saikhowa National Park area due to avulsion from 1955 to 2019 (figure 7). For that, the toposheet has been geo-referenced before extracting vector layers. Imageries are digitised and drainage is extracted to vector layers for measuring areas, perimeters and lengths.

CartoDEM, IRS P6 LISS-III and Google Earth Pro satellite data are used to delineate the extent of palaeostream within the IDB area (figures 8 and 9).

4. Results

The results of the morphometric analyses using three categories of parameters, viz., relief, aerial and tectonic as listed in table 1 for Burhi Dihing river

Table 1. *Parameters selected for morphometric analyses in the composite drainage basin of Noa Dihing, Burhi Dihing and the Dibru river.*

Category	Parameter	Formula	Description
Relief	Total basin relief (H) (Strahler 1952)	$H = H_{\max} - H_{\min}$	$H_{\max}$ = Maximum elevation $H_{\min}$ = Minimum elevation
	Relief ratio (Rh) (Schumm 1956)	$Rh = H/Lb$	H = Basin relief Lb = Basin length
	Relative relief (Rhp) (Melton 1957)	$Rhp = H \times 100/P$	H = Basin relief P = Basin perimeter
Aerial	Form factor (Rf) (Horton 1932)	$Rf = A/Lb^2$	A = Area of the basin Lb = Basin length
	Circularity index (Rc) (Miller 1953)	$Rc = 4\pi A/P^2$	Ratio between basin area (A) to the area of a circle having the same circumference as the perimeter (P) of the basin
	Elongation ratio (Re) (Schumm 1956)	$Re = Dc/Lb = \sqrt{4A/\pi}/Lb$	Dc is the diameter of the circle of the same area as the basin
Tectonic	Hypsometric integral (Hi) (Strahler 1952; Bull and McFadden 1977)	$Hi = \frac{H_{\text{mean}} - H_{\min}}{H_{\max} - H_{\min}}$	H_{mean} = mean elevation, $H_{\min}$ = minimum elevation $H_{\max}$ = maximum elevation
	Mountain-front sinuosity (Smf) (Bull and McFadden 1977)	$Smf = Lmf/Ls$	Lmf = length of the mountain front along the mountain piedmont junction, Ls = straight-line length of the mountain
	Asymmetry factor (AF) (Cox 1994; Keller and Pinter 2002)	$AF = \frac{Ar}{A} \times 100$	Ar = right-hand side area of drainage looking downstream
	Transverse topographic symmetry (T) (Cox 1994)	$T = \frac{Da}{Dd}$	Da is the distance from the active *meander-belt midline* to the *basin midline*, Dd = the distance from the *basin divide* to the *basin midline* as depicted in simplified diagram

Table 2. *Results of morphometric analyses of parameters under relief category.*

	Parameters									
Drainage basins	Perimeter (P) (km)	Basin length (Lb) (km)	Basin area (A) (km^2)	Surface area 3D (S) (km^2)	Max elev. ($H_{\max}$) (km)	Min elev. ($H_{\min}$) (km)	Basin relief (H) (km)	Hypso-metric integral (Hi)	Relief ratio (Rh)	Relative relief (Rhp)
BDB	512.01	191.97	5874.3	6055.9	2.766	0.091	2.675	0.005	13.934	522.450
DB	157.3	64.51	585.02	585.13	0.196	0.110	0.086	−0.17	1.333	54.672
NDB	459.11	176.17	3486.9	3711.4	4.327	0.117	4.210	0.023	23.867	916.991

basin (BDB), Dibru river basin (DRB) and Noa Dihing river basin (NDB) are presented in tables 2–5. Parameters such as basin relief (H), relief ratio (Rh) and relative relief (Rhp) of relief aspects are shown in table 2. Table 3 represents analyses results of parameters form factor (Rf), circularity index (Rc), elongation ratio (Re) and asymmetry factor (AF). The calculations for the determination of mountain front sinuosity (Smf) are given in table 4. The changes observed in perimeter and area in the Dibru Saikhowa area in the time period of 45 years from 1974 to 2019 are shown in table 5.

Table 3. *Results of morphometric analyses of Rf, Rc, Re and AF of aerial and tectonic categories.*

	Parameters				
Basins	Form factor (*Rf*)	Circularity index (*Rc*)	Elongation ratio (*Re*)	RHS area of the drainage basin (*Ar*) (km^2)	Asymmetry factor (*AF*)
BDB	0.159	0.282	0.450	2473.9	42.11
DB	0.141	0.297	0.422	167.54	28.64
NDB	0.112	0.208	0.378	2147.7	61.59

Table 4. *Results of morphometric analyses of mountain-front sinuosity (Smf).*

	Parameters					
Basins	Length of mountain front along piedmont junction (Lmf_1)	Length of mountain front along piedmont junction (Lmf_2)	Straight line length of the mountain (Ls_1)	Straight line length of the mountain (Ls_2)	Mountain-front sinuosity (Smf_1)	Mountain-front sinuosity (Smf_2)
BDB	140	250	37.065	88.082	3.777	2.838
DB	140	20	155	23	0.903	0.869
NDB	200	400	24.388	23.608	8.200	16.943

4.1 *Relief aspects*

4.1.1 *Basin relief*

Table 2 presents results of morphometric analyses for the BDB, DB and NDB of relief category using 2019 Landsat 8 OLI images. H_{max} and H_{min} for BDB are 2766 and 91 m, for DB are 196 and 110 m, and for NDB are 4327 and 117 m, respectively. Therefore, the reliefs (*H*) of BDB, DB and NDB are found 2675, 86 and 4210 m, respectively. This suggests that catchment areas of BDB and NDB are located in higher altitude than the rest of the valley area. Some portions of the catchment area of NDB fall in the Mishmi Hills, which is the easternmost extension of the Arunachal Himalaya. On the contrary, the basinal area of DB is confined to the valley only; therefore, the *H* value of DB is significantly lower than the rest of the two basins. This also suggests that DB has no such catchment area like the NDB and the BDB.

4.1.2 *Relief ratio*

Relief ratio (*Rh*) values of these basins (table 2) are 13.934 (for BDB), 1.33 (for DB) and 23.867 (for NDB). It means that NDB and BDB have higher slope gradients than DB as their catchment areas are located at higher elevations. The lower value of *Rh* also supports the fact that DB does not have a catchment area like NDB and BDB.

4.1.3 *Relative relief*

Rhp values of these basins are 522.45, 54.67 and 916.991 for BDB, DB and NDB, respectively (table 2). It means distribution of the catchment area of NDB is located at much rougher terrain than the rest of these two basins, and the basin configuration of DB is significantly flatter than BDB and NDB.

4.2 *Aerial aspects*

4.2.1 *Form factor*

As listed in table 3, the *Rf* values of BDB, DB and NDB are obtained as 0.159, 0.141 and 0.112, respectively. As these values are less than 1, all the three basins are elongated.

4.2.2 *Circularity index*

The *Rc* values calculated for BDB, DB and NDB are 0.282, 0.297 and 0.208, respectively (table 3). These suggest that all these basins are elongated in shape rather than circular.

Table 5. *Total loss in perimeter (in km) and area (in km^2) of Dibru Saikhowa in last 45 years (1974–2019) from the analyses of Landsat imageries.*

Sl. no.	Time of imagery	Perimeter (km)	Loss/grain in perimeter (km)	Enclosed area (km^2)	Loss/grain in area (km^2)	Sensor type	Remark
1	Jan-1974	135.58		475.85		Landsat 15 MSS	DR and DgR present, LR flowing on north of DS
2	Jan-1988	115.17	−20.41	439.79	−36.06	Landsat 4–5 TM	Same
3	Oct-1992	107.5	−7.67	359.83	−79.96	Landsat 4–5 TM	High Q through DgR and DR
4	Nov-1994	105.82	−1.68	349.5	−10.33	Landsat 4–5 TM	Diversion of Q from LR towards DR and high Q in DR
5	Dec-1996	161.86	+56.04	366.38	+16.88	Landsat 4–5 TM	Q from DbR and LR are diverting through DR via DgR
6	May-1998	112.34	−49.52	339.82	−26.56	Landsat 4–5 TM	Same
7	Oct-2000	121.38	+9.04	356.36	+16.54	Landsat 4–5 TM	Same
8	Nov-2005	120.94	−0.44	311.37	−44.99	Landsat 4–5 TM	DbR changed the course towards DhR, i.e., north of DS
9	Sep-2006	114.4	−6.54	292.36	−19.01	Landsat 4–5 TM	High Q in all streams
10	Nov-2008	112.48	−1.92	307.24	+14.88	Landsat 4–5 TM	Small connection between DbR and LR
11	Nov-2016	109.94	−2.54	272.62	−34.62	Landsat 8 OLI	Same
12	Jan-2019	105.88	−4.06	271.81	0.81	Landsat 8 OLI	Same
Total	(in 45 years interval)		−29.7		−204.04		

DR: Dibru river, DgR: Dangori river, LR: Lohit river, DbR: Dibang river, DS: Dibru Saikhowa, Q: water discharge, DhR: Dihang river.

4.2.3 *Elongation ratio*

Similarly, *Re* values determined for these basins (table 3) are 0.45, 0.422 and 0.378, respectively. The *Re* values also inferred that the shape of these three drainage basins, viz., NDB, BDB and DB are elongated. Especially the shape of NDB is more elongated than the rest of the two.

4.3 *Tectonic aspects*

4.3.1 *Hypsometric integral*

Under the tectonic aspects, the values of hypsometric integral (*Hi*) for the BDB, DB and NDB basins are calculated as (table 2) 0.005, 0.17 and 0.023, respectively. It suggests that out of these two basins, DB has an old eroded landscape and NDB has comparatively a new drainage basin.

4.3.2 *Mountain-front sinuosity*

Mountain-front sinuosity (*Smf*) measured at two different elevation levels, i.e., Smf_1 at 150 m and Smf_2 at 200 m elevations are listed in table 4. Smf_1 for BDB, DB and NDB are 3.77, 0.903 and 8.2, respectively. Smf_2 for BDB, DB and NDB are 2.838, 0.869 and 16.943, respectively. It suggests that the expression of mountain-front for BDB and NDB are significantly rough as they have direct influence of active thrust zone, i.e., NT located within 1–3 km distance. The *Smf* value closer to 1 suggests a smooth expression. A high value of *Smf* indicates significant variation in the length of the mountain front along the piedmont junction (*Lmf*). The values of *Smf* for BDB and NDB are >1, which suggest strong tectonic control in the development of the basin. The presence of the Naga hills (marked by NT and DT towards the SE frontier) has affected the *Smf* of these basins.

4.3.3 *Asymmetric factor*

Asymmetric factor (AF) calculated for BDB, DB and NDB are 42.11, 28.64 and 61.59, respectively (table 3). If the value of asymmetry factor (AF) is ∼50, the basin is symmetric and both sides have an equal area. AF values suggest that there are certain topographic controls over the flow directions of the rivers. Neotectonic uplift on one side of the basin may affect the AF values. Therefore, all three basins have moderate degree of asymmetry.

4.3.4 *Transverse topographic symmetry*

Transverse topographic symmetry (T) vectors calculated for NDB, DB and BDB are shown in figure 6(a–c), respectively. In a completely symmetric basin transverse topographic symmetry, $T = 0$ and as asymmetry increases T approaches a value of 1.0 (Salvany 2004). Note the central part of the NDB receives a moderate southern shift. DB, on other hand, shows shift towards the south at the western part of the basin and reverse eastern shift at the central part. In the case of the NDB, moderate northern shift is observed at the segment which is flowing parallel to the NT at Digboi anticline. However, towards the terminal side of the basin, opposite shifting has been observed.

4.4 *Avulsion and formation of Dibru Saikhowa river island*

Comparing the 1955 US Army Toposheet with the recent satellite imageries reveals that the area of IDB containing NDB, DB and BDB (figure 7i–iii) was ∼4552 km^2 ∼60 years ago and is currently ∼3835 km^2 with a perimeter of ∼445 km. Within a period of ∼60 years, the track of Lohit has been diverted through Dangori river (a tributary of the Dibru river) near the Sadia. As a result, a segment of the Dibru river also vanished from Guijan to Rahmoria (near Sadia) and became a part of the Lohit river (figure 7i and ii). The gradual shifting of flow of Lohit via a course of Dangori has already been reported (Sarma 2005; Sarma *et al.* 2011) and can be observed in the time-lapsed satellite images (figure 7A–H). Shifting occurred mainly between the years 1992 and 1994. In this period, Lohit captured (avulsion) a segment of the Dibru river (Borgohain *et al.* 2016; Mather *et al.* 2002). Therefore, a huge landmass, called Dibru Saikhowa, is now surrounded by rivers – Lohit at SE and Dihang and Dibang at NW. Thus, the detached landmass has become a part of the Brahmaputra (figure 7H). The present-day area of the Dibru Saikhowa National Park, now a river island, is ∼250 km^2 in area. Comparing the earlier drainage networks with the present-day scenario reveals that 467 km^2 of area has been lost in this period due to bank erosion, channel shifting, river capturing and avulsion. GIS-based measurements as given in table 5 show steps involved in the transformation of this landmass into a river island due to river capturing. Around 1992, discharge from Lohit interfered with the course of the Dangori river, and gradually widened the width within 4–5 years. The confluence point of the Lohit changed from the north of Dibru Saikhowa to 8.64 km south side and diverted its flow through Dangori river. Borgohain *et al.* (2016) reported that the topographic elevations have an effect on the channel shifting of the Lohit river. The presence of several sub-surface normal faults at the basement of the Brahmaputra arch (Kumar *et al.* 2012) below the study area may trigger a lateral change in gradients. Tectonic controls over the drainage systems of the Brahmaputra have been previously reported by many authors, e.g., Sarma (2005), Das and Saraf (2007), Sarma *et al.* (2011), Lahiri and Sinha (2012) and Bracciali *et al.* (2015).

4.5 *Formation of palaeostreams and misfit streams*

The IDB contains small streams Dibru and Dangori river (relict stream segment, figures 7(i–ii) and 8, that are fed by further small tributaries such as Doom Dooma river, Maila Jan, Kav Jan, Maran Jan and Dekia Jan. A close observation of satellite imagery and Carto DEM (figure 8) reveals that the Dibru river (50–70 m wide) flows through valleys, which is ∼1–2 km wide. The valley is quite larger in size for the stream, and therefore Dibru river can be regarded as a misfit stream (Lake and Rastall 1910; Harris 1997; Roy and Sinha 2005). An impression (figures 8 and 9) of a 145 km long palaeostream (locally known as Maijan), covering an aerial distance of ∼88 km is present between Tingrai area to Bongal Gaon (figure 9).

Carto DEM (figure 8) indicates that the drainage of the Dibru river was quite large at some time range. Progressively it became a small stream. Along with these small drainages, there is an impression (figure 9) of a 145 km long palaeo-stream

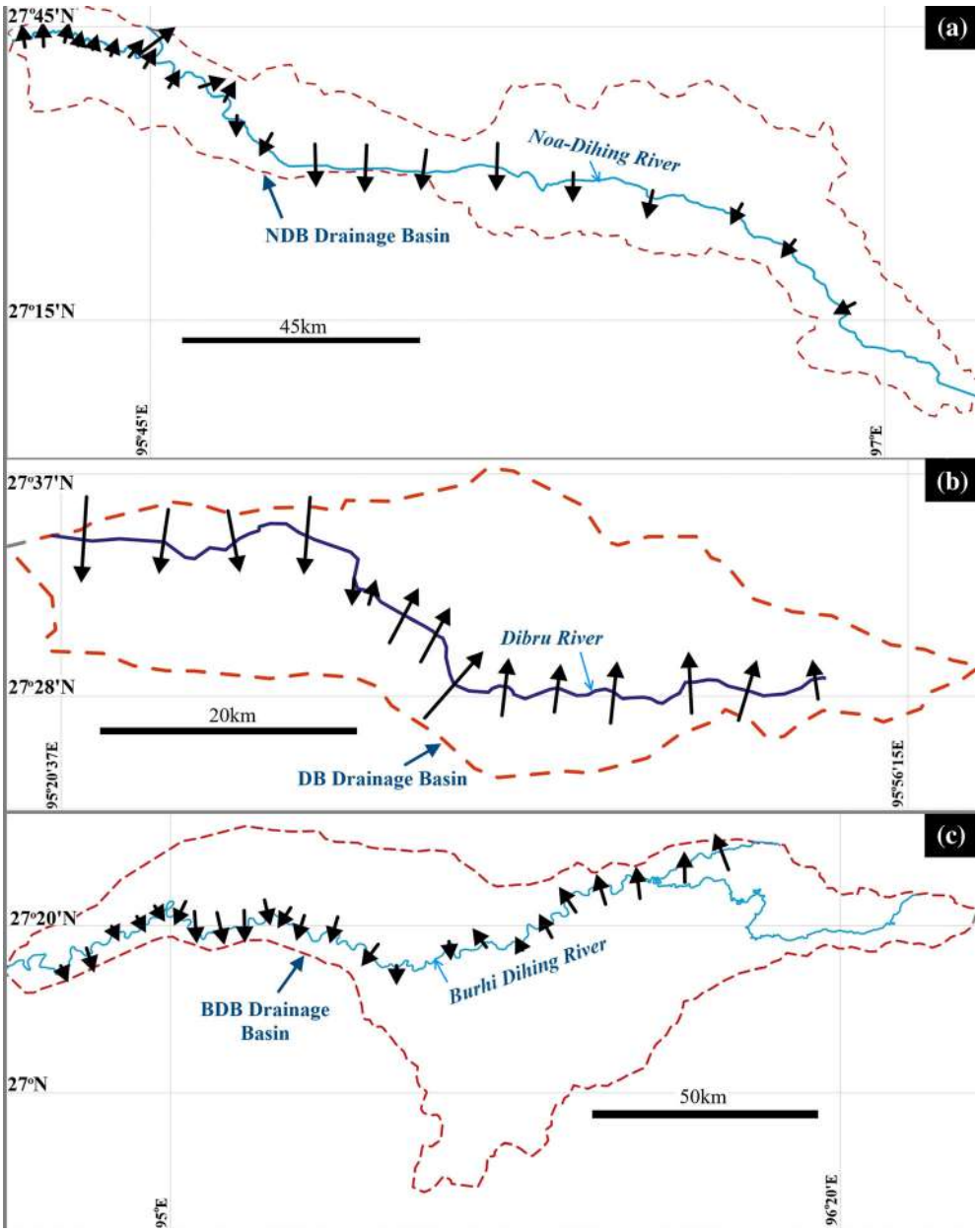

Figure 6. Transverse topographic symmetry, T (Cox 1994) vectors calculated for (**a**) NDB, (**b**) DB and (**c**) BDB are shown.

locally known as Maijan, covering an aerial distance of ∼88 km from Tingraito Bongal Gaon, near the Mohanbari area in Dibrugarh. Near the Tingrai area the paleo-impression of Dibru river is observed near Maijan (figure 9) as having the same water-head splitting into two different streams, which suggests channel diversion in the past. From Namphuk to Pawoimukh (figure 2), the river Burhi Dihing flows through a foredeep basin (Mikhailov *et al.* 1999) developed in the hanging wall of the NT (Kent *et al.* 2002). The trail of the Maijanpalaeostream has been traced in the Tingrai area near Barjan (figure 9). Digboi (at Digboi anticline) is located a few kilometres SE of Barjan (figure 8). Therefore, the rise of the anticline must have detached the feeding tributaries of Maijan towards SW of the foredeep. This change resulted in gradual drying of Maijan due to insufficient discharge. Figure 10 presents the possible scenario existed before and after anticlinal uplift. The average width of Mai Jan paleo-stream, which is about ∼230 km, is equivalent to the width of the present Burhi Dihing river (∼205 km). It indicates that Mai Jan was once a dominant stream in this basin. Later it is detached from the headwater stream and dried up, which could be by neotectonic uplift of the SE part of the basin followed by channel diversion towards Dibru river. The river is also

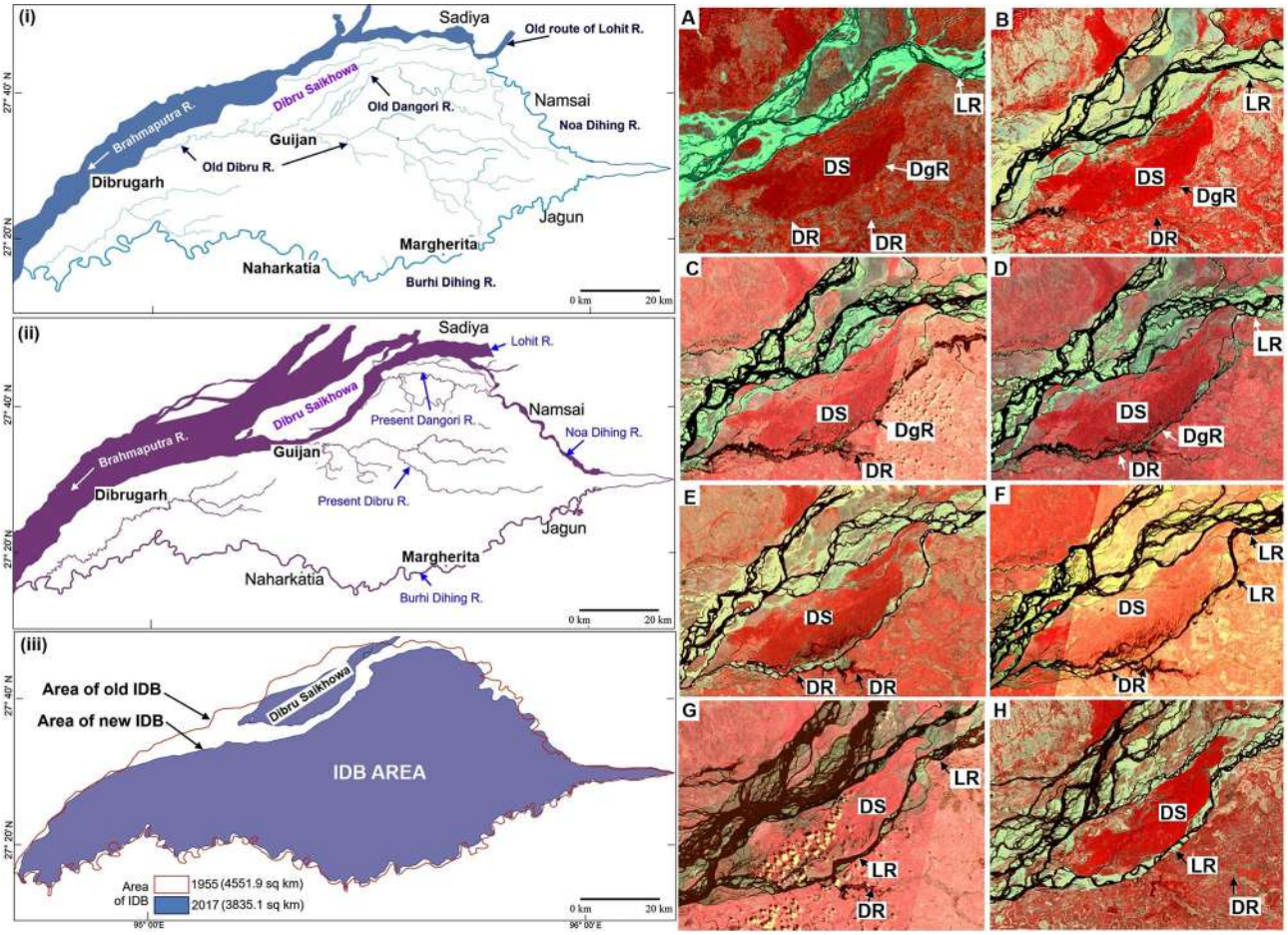

Figure 7. (**i**) Drainage network before 1955 as found in the US Army Map no. NG 46-4, of series U502 Edition 1-AMS (1957) prepared by Army Map Service (PV), Corps of Engineers, US Army, Washington, DC, Compiled in 1955 from: India, 1:63360, Survey of India (edition 1918–1934), 1:126,720, Survey of India (1927–1929), (**ii**) drainage of 2017–2018 traced from Google Earth imageries, and (**iii**) comparison between area of IDB. (**A**) Jan-1974 (Landsat 1–5 MSS), (**B**) Jan-1988 (Landsat 4–5 TM), (**C**), Oct-1992 (Landsat 4–5 TM), (**D**) Nov-1994 (Landsat 4–5 TM), (**E**) Dec-1996 (Landsat 4–5 TM), (**F**) May-1998 (Landsat 4–5 TM), (**G**) Sep-2006 (Landsat 4–5 TM), (**H**) Jan-2019 (Landsat 8 OLI).

gradually drying and converting into a misfit stream.

5. Discussion

Morphometric analyses of these three basins suggest that NDB and BDB are elongated and have catchment areas located at elevated regions. Elongated shape may be related to structural controls over the drainage basin (Prakash *et al.* 2017; Manjare *et al.* 2020). Relief analyses show that except DB, the other two basins, viz., NDB and BDB are experiencing active drainage due to the presence of the catchment area located in adjacent high elevated terrain. The area of DB is significantly small in spite of having a valley larger than the river (figure 8). DB does not possess such catchment area, which is unusual to tributaries of Brahmaputra because all of the tributaries originate from either the Himalayas or Naga Hills (figure 2). However, the area of DB is confined to the valley alone. The presence of traces of palaeo-stream connected to the Dibru river near Digboi (figure 9) and the Maijanpalaeo-stream (figure 8) suggests that the emergence of the Digboi anticline (due to propagation of NT) blocked the headwater (figure 10) from the Naga Hills and detached the discharge. Gradually both rivers have dried due to lack of sufficient discharge leaving behind only the dry river valley. Later the discharge diverted to the present day Burhi–Dihing river. *Smf* calculations of the BDB and NDB clearly show that the expression of mountain front is rough. NT has not only created a foredeep south of Digboi anticline (through which Burhi–Dihing is presently flowing) but detached the previous drainage connections of Maijan and Dibru river from its headwater

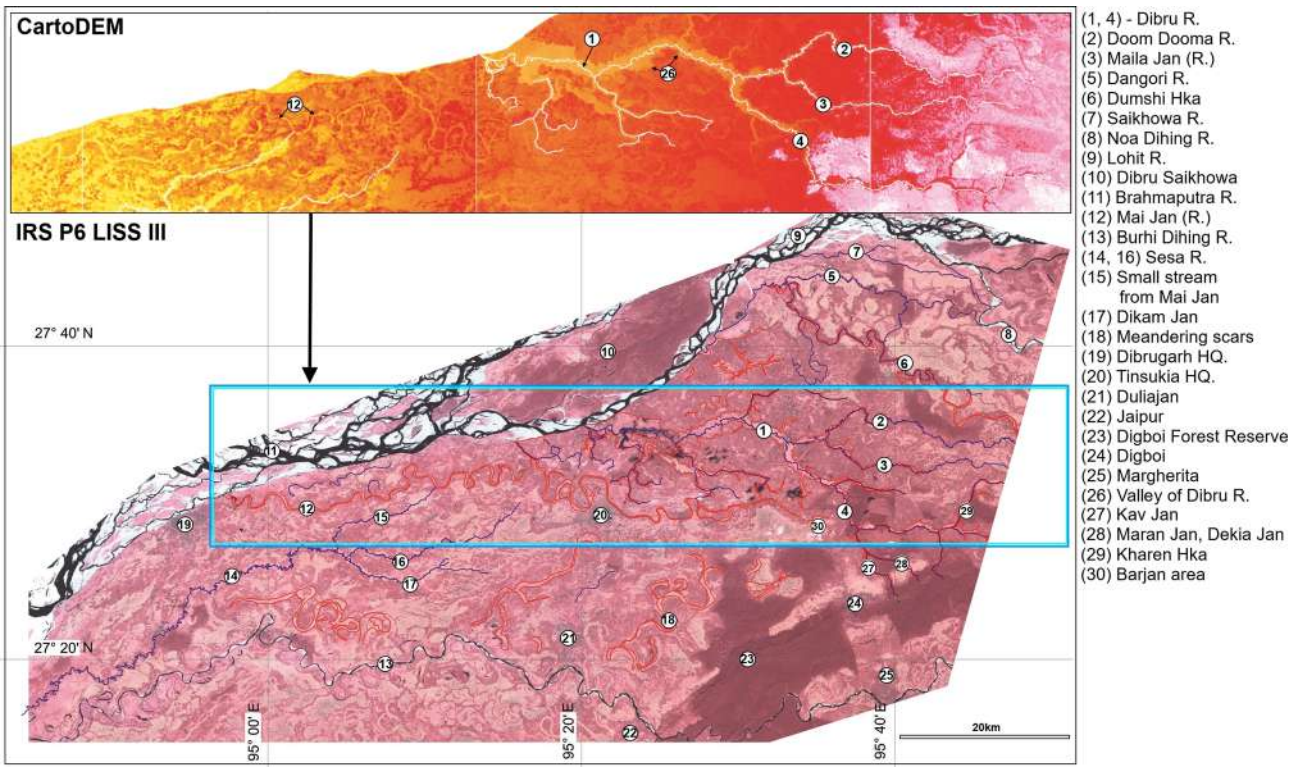

Figure 8. Palaeo-river segments and meandering scars (in red) and other small rivers (in indigo) exist in the basin (IRS P6 LISS III imagery) inset showing CartoDEM indicating relief trace of Maijan palaeostream (12) and valley of Dibru river (26).

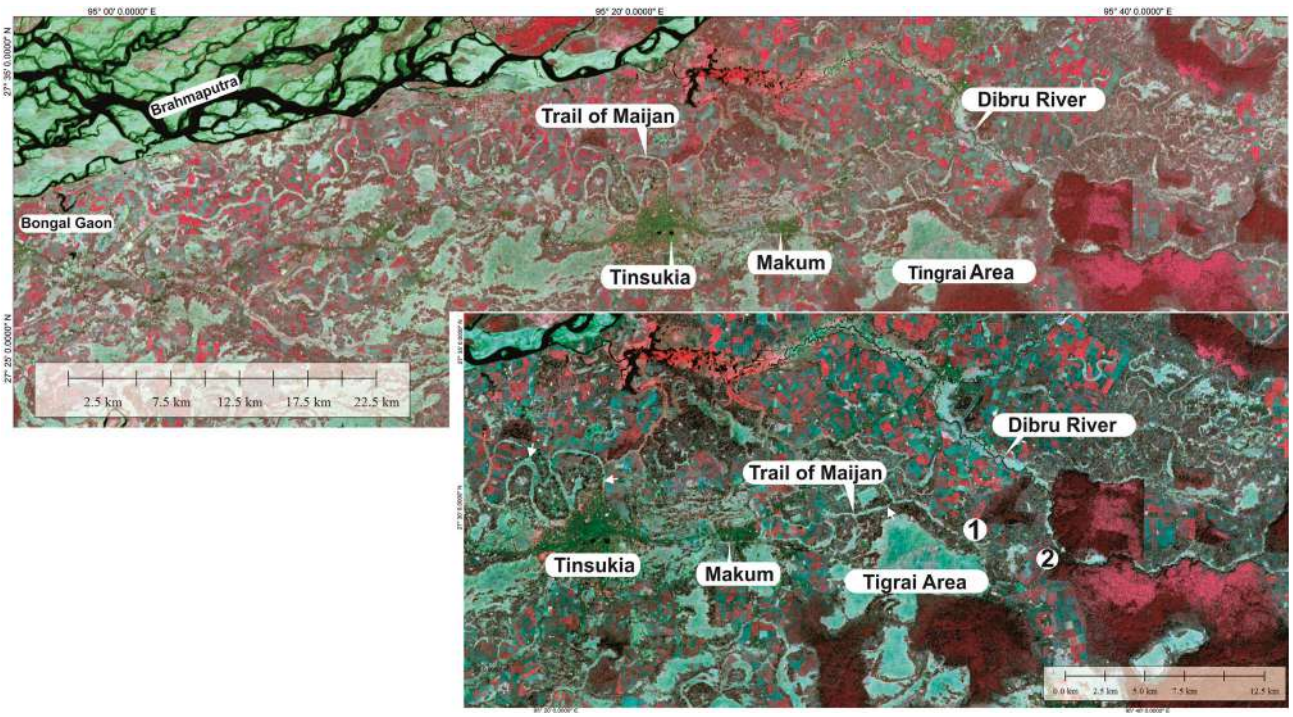

Figure 9. Trail of Maijan originating from (1) Tokowani village, near Tingrai and ending at Brahmaputra near BogalGaon, near Mohanbari, Dirbugarh and a few metres ahead east of the existing Dibru river and (2) Bogapani Tea Estate (Google Earth imageries).

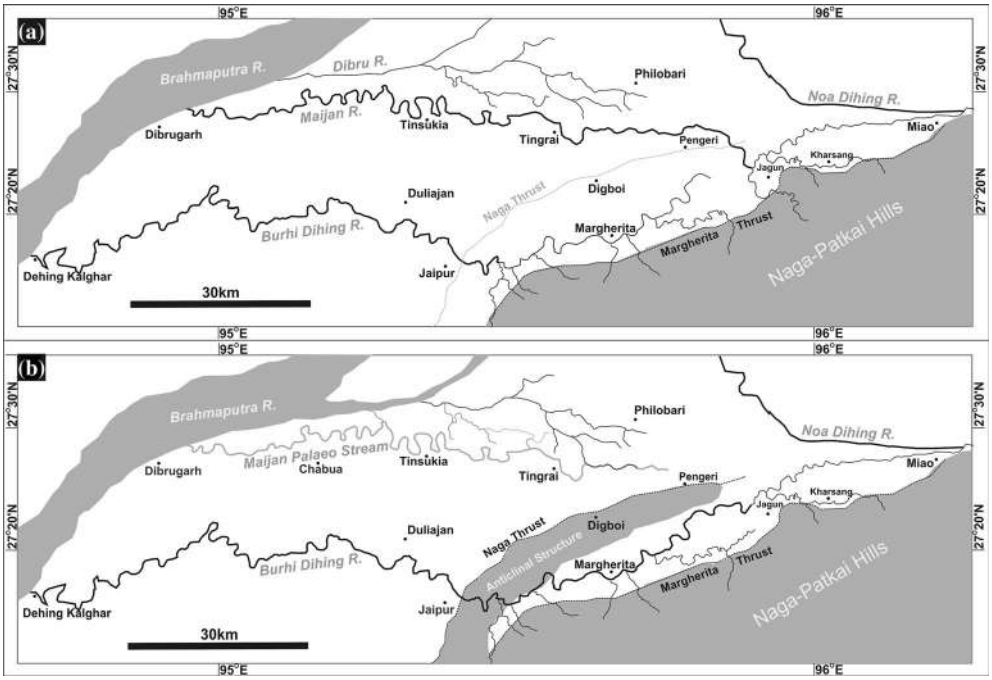

Figure 10. Schematic model of formation of Maijanpalaeo stream due to the rise of Digboi anticlinal structure induced by NT. (**a**) Pre-uplift possible flow of the Maijan and Burhi Dihing river prior to the activation of NT, and (**b**) post uplift present-day flow of Burhi Dihing and palaeo remains of Maijan. In the foredeep behind NT and DT, Burhi Dihing is flowing along the MgT (Margherita thrust).

supplying tributaries (figure 10). This is a major fluviological change that had occurred due to tectonic movement in recent past.

The satellite record of the last 45 years (figure 7) and changes observed in the perimeter and total area of the Dibru Saikhowa landmass from the satellite data (table 5) show a major shift in channel segment of Lohit. Around 1992, the Lohit river interfered with the course of the Dangori river, and diverted 8.64 km towards south. This might be related to the change in profile gradient (Borgohain *et al.* 2016). The movement along the fault systems of the Brahmaputra arch at the basement probably modified the gradient. Similarly, neotectonic movement in thrust systems located at the foothill ranges of the Himalayas in the north of the study area may also affect the gradients. Tectonic controls over the drainage systems of the Brahmaputra have been previously reported by many authors viz., Sarma (2005), Das and Saraf (2007), Sarma *et al.* (2011), Lahiri and Sinha (2014) and Bracciali *et al.* (2015). *AF* of NDB shows a moderate degree of asymmetry. Transverse topographic symmetry of these basins also shows that the western part of the Dibru river, which is connected with the Lohit river has a southern shift (figure 6). The reverse shift in the eastern and central segments of the Dibru river can also be observed in the western part of Noa Dihing. The southern shift of Noa Dihing could be attributed to the uplift on the north of the basin.

6. Conclusions

Morphometric analyses of the IDB consisting of NDB (Noa Dihing Basin), DB (Dibru Basin) and BDB (Burhi Dihing Basin) have neotectonic effects.

(a) Higher values of *H*, smaller values of *Rh* and high *Rhpi* indicate higher gradients due to the presence of elevated catchment in BDB and NDB. However, DB is a basin, which has been detached from such catchment areas due to tectonic activities.

(b) All three basins are elongated in shape, as shown by the analyses of parameters (*Rf*, *Rc* and *Re*) of aerial aspects. NDB especially has higher degree of structural control and therefore affects basin shape.

(c) *Hi* values suggest that DB has an old drainage landscape. *Smf* study indicates that the presence of NT and other thrust affects expression of mountain-front towards south of the valley.

AF and *T*-vectors (figure 6) suggest that all three basins have moderate degree of asymmetry and shift due to active tectonics.

(d) Formation of palaeostreams and misfit rivers in recent past due to the emergence of fault propagation fold (Digboi anticline) attributed by the propagation of NT (figure 10).

(e) Change in the course of the Lohit river from the western side to the eastern side of the Dibru Saikhowa National Park in the last 25 years (figure 7) and the formation of river island may be associated with change in channel gradient due to subsurface fault movement at the basement arch, or due to the uplift of basin towards the northern side.

Typical tectonic setting of the Assam valley makes it a tectonically active region. Frequent occurrences of earthquakes along the nearby fault systems due to the neotectonics may create risk to the lives of inhabitants of small township areas, e.g., Tinsukia, Dibrugarh and Doom Dooma, as well as can cause failure of major engineering projects, e.g., bridges, dams; and most worryingly various coal- and oil-field structures. Surface features are a result of endogenic dynamics and lithospheric tectonics, and fluvial features are the most sensitive to such factors. This study gives the clue to neotectonic changes that had occurred over the last few decades and brought changes to the fluvial systems. Recognition and morphometric analyses of such fluvial changes can provide evidences of neotectonic activities resulting from plate movements and can upgrade understanding of future possibilities or changes that could be brought into the system. In summary, predictive geomorphic models of this terrain therefore will be the next step for research studies.

Acknowledgements

SM was supported by CPDA grant of IIT Bombay. Authors thank the Chief Editor, associate editor, reviewers, managing editor and proofreaders.

Author statement

Manash Pratim Gogoi: Working with software, writing of the original draft. Bikash Gogoi: Supervision. Soumyajit Mukherjee: Supervision, revision of the draft.

References

Aier I, Luirei K, Bhakuni S S, Thong G T and Kothyari G C 2011 Geomorphic evolution of Medziphema Intermontane basin and Quaternary deformation in the Schuppen belt, Nagaland, NE India; *Zeits. Geomorphol.* **55** 247–265.

Alam J, Chatterjee R and Dasgupta S 2019 Estimation of pore pressure, tectonic strain and stress magnitudes in the upper Assam basin: A tectonically active part of India; *Geophys. J. Int.* **216** 659–675.

Angelier J and Baruah S 2009 Seismotectonics in northeast India: A stress analysis of focal mechanism solutions of earthquakes and its kinematic implications; *Geophys. J. Int.* **178** 303–326.

Babu P V L P 1994 Neotectonic events and hydrocarbon plays in the sedimentary basins of India; In: *Proceedings of the second seminar on petroliferous basins of India: East coast, Andaman and Assam–Arakan Basins,* Vol. **3** (eds) Biswas A K, Pandey A, Dave A, Maithani A, Garg P and Thomas N J, Indian Petroleum Publishers, Dehradun, pp. 237–240, ISBN 81-900361-0-6.

Biswas A K, Pandey A, Dave A, Maithani A, Garg P and Thomas N J 1993 *Proceedings of the second seminar on petroliferous basins of India: East coast, Andaman and Assam–Arakan Basins*; Indian Petroleum Publishers, Dehradun, Vol. **3**, pp. 1–46, ISBN 81-900361-0-6.

Borgohain S, Das J, Saraf A K, Singh G and Baral S S 2016 Morphodynamic changes of Lohit River, NE India: GIS-based study; *Curr. Sci.* **110(9)** 1810–1816.

Borgohain S, Das J, Saraf A, Singh G and Baral S S 2017 Structural controls on topography and river morphodynamics in Upper Assam Valley, India; *Geodinamica Acta* **29(1)** 62–69.

Bracciali L, Najman Y, Parrish R P, Akhter S H and Millar I 2015 The Brahmaputra tale of tectonics and erosion: Early Miocene river capture in the eastern Himalaya; *Earth Planet. Sci. Lett.* **415** 25–37.

Bull W B and McFadden L M 1977 Tectonic geomorphology north and south of the Garlock fault, California; *J. Geomorphol.* **1** 15–32.

Chopra S 1980 A note on the avulsion of Ranga river, district north Lakhimpur, Assam, photo nirvachak; *J. Ind. Soc. Photo-Interpret. Remote Sens.* **8** 59–61.

Conybeare C E B 1976 Geomorphology of oil and gas fields in sandstone bodies; In: *Developments in Petroleum Science 4*, Elsevier, Amsterdam, 296p, ISBN 0444-41398-7.

Cox R T 1994 Analysis of drainage basin asymmetry as a rapid technique to identify areas of possible Quaternary tilt-block tectonics: An example from the Mississippi embayment; *Geol. Soc. Am. Bull.* **106** 571–581.

Das D 2014 'Majuli in Peril': Challenging the received wisdom on flood control in Brahmaputra river basin, Assam (1940–2000); *Water History* **6** 167–185.

Das J D and Saraf A K 2007 Technical note: Remote sensing in the mapping of the Brahmaputra/Jamuna river channel patterns and its relation to various landforms and tectonic environment; *Int. J. Remote Sens.* **28** 3619–3631.

Das Gupta A B and Biswas A K 2000 *Geology of Assam*; GSI Publications, Bangalore, ISBN-13:978-818586744110.

Dasgupta S, Pande P, Ganguli D, Iqbal Z, Sanyal K, Venkataraman N V, Dasgupta S, Sural B, Harendranath L, Mazumdar K, Sanyal S, Roy A, Das L K, Misra P S and

Gupta H 2000 *Seismotectonic atlas of India and its environs* (eds) Narula P L, Acharyya S K and Banerjee J, Geol. Surv. India, Bangalore.

Deb S S, Barua I and Sarma B P 2012 Prospects exploration and future exploration strategy in Paleocene/Eocene formations of basement high and adjoining areas in upper Assam basin based on paleoenvironment; *Assoc. Petrol. Geol. Bull.* **8** 61–70.

Deshpande S V, Goel S M, Bhandari A, Baruah R M, Deshpande J S, Kumar A, Rana K S, Chitrao A M, Giridhar M, Chowdhuri D, Kale A S and Phor L 1993 *Lithostratigraphy of Indian Petroliferous Basins, Document* – X. Unpubl. Report ONGC, 122p.

Dutta P and Konwar M 2013 Morphological aspects of floodplain wetlands with reference to the upper Brahmaputra river valley; *Int. J. Sci. Res. Publ.* **3(9)**, ISSN 2250-3153.

Dwivedi K K 2016 Journey, Flood and River Erosion Management Agency of Assam (FREMAA); http://thebrahmaputra.in/jour.php.

Evans P 1932 Tertiary succession in Assam; *Trans. Min. Geol. Inst. Ind.* **5** 155–260.

Ghosh G K, Basha S K, Salim M and Kulshreshtha V K 2010 Integrated interpretation of seismic, gravity, magnetic and magneto-telluric data in geologically complex thrust belt areas of Manabum, Arunachal Pradesh; *J. Ind. Geophys. Union* **14** 1–14.

Gogoi C and Goswami D C 2014 A study on channel migration of the Subansiri river in Assam using remote sensing and GIS technology; *Curr. Sci.* **106** 1113–1120.

Goswami A B 1984 Environmental geoscientific appraisal of upper Brahmaputra valley; *Ind. Miner.* **38** 28–36.

Goswami U and Acharjee S 2016 Anabranches of the Subansiri in Assam, India: The unsolved enigma of an alluvial river; *South East Asian J. Sedim. Basin Res.* **2–4** 13–22 (ISSN 2320-6829).

Handique G K, Sethi A K and Sarma S C 1989 Review of tertiary stratigraphy of parts of upper Assam valley; *Geol. Surv. India Spec. Publ.* **23** 23–36.

Harris S A 1997 Misfit stream; In: *Encyclopedia of Earth Science* (ed.) Geomorphology, Springer, Berlin, Heidelberg, https://doi.org/10.1007/3-540-31060-6_243.

Heidbach O, Rajabi M, Reiter K, Ziegler M and WSM Team 2016 World Stress Map Database Release 2016; V. 1.1. GFZ Data Services, https://doi.org/10.5880/WSM.2016.001.

Horton R E 1932 Drainage-basin characteristics; *Eos, Trans. Am. Geophys. Union* **13**.

Keller E A and Pinter N 2002 *Active tectonics: Earthquakes, uplift, and landscape*; Prentice Hall, Upper Saddle River, NJ, 362p.

Kent W N and Dasgupta U 2004 Structural evolution in response to fold and thrust belt tectonics in northern Assam: A key to hydrocarbon exploration in the Jaipur anticline area; *Mar. Pet. Geol.* **21** 785–803.

Kent W N, Hickman R G and Dasgupta U 2002 Application of a ramp/flat-fault model to interpretation of the Naga thrust and possible implications for petroleum exploration along the Naga thrust front; *AAPG Bull.* **86** 2003–2045.

Kumar S T, Bharali B R and Verma A K 2012 Basement configuration and structural style in OIL's operational areas of Upper Assam; *AAPG Online Journal for E&P Geoscientist*, https://www.searchanddiscovery.com/documents/2012/50739kumar/ndx_kumar.pdf.

Kunte S V 1988 Geomorphic analysis of upper Assam plains and adjoining areas for hydrocarbon exploration; *J. Ind. Soc. Remote Sens.* **16(1)** 15–28.

Lahiri S K and Sinha R 2012 Tectonic controls on the morphodynamics of the Brahmaputra river system in the upper Assam valley, India; *Geomorphology* **169–170** 74–85.

Lahiri S K and Sinha R 2014 Morphotectonic evolution of the Majuli Island in the Brahmaputra valley of Assam, India inferred from geomorphic and geophysical analysis, *Geomorphology* **227** 101–111, https://doi.org/10.1016/j.geomorph.2014.04.032.

Lake P and Rastall R H 1910 A Text-Book of Geology, Edward Arnold, London, 1st edition, pp. xvi + 494.

Manjare B S, Singh V and Masurkar S P 2020 Tectonic control on drainage network evolution and evidence of neotectonic activities in the Wan river sub-basin, central India; IOP Conf. Series, *Earth Environ. Sci.* **597**.

Malik J N and Mohanty C 2007 Active tectonic influence on the evolution of drainage and landscape: Geomorphic signatures from frontal and hinterland areas along the northwestern Himalaya, India; *J. Asian Earth Sci.* **29** 604–618.

Mather A E, Stokes M and Griffiths J S 2002 Quaternary landscape evolution: A framework for understanding contemporary erosion, SE Spain; *Land Degrad. Manag.* **13** 1–21.

Mathur L P and Evans P 1964 Oil in India; 2nd Int. Geol. Congr., New Delhi, 85p.

Mathur N, Raju S V and Kulkarni T G 2001 Improved identification of pay zones through integration of geochemical and log data: A case study from Upper Assam Basin, India; *AAPG Bull.* **85(2)** 309–323.

Mazumder S, Dave H D, Samal J K and Mitra D S 2012 Delineation of basement-related fault closures in eastern part of Purnea basin based on morphotectonic analysis; *Assoc. Petrol. Geol. Bull.* **8** 41–47.

Melton M 1957 An analysis of the relations among elements of climate, surface properties and geomorphology; Department of Geology, Columbia University, Technical Report, 11, Project NR 389-042. Office of Navy Research, New York.

Mikhailov V O, Timoshkina E P and Polino R 1999 Foredeep basins: The main features and model of formation; *Tectonophys.* **307** 345–359.

Miller V C 1953 A quantitative geomorphic study of drainage basin characteristics in clinch mountain area, Virginia and Tennessee; Technical report, 3, Office of the Naval Research. Dept. Geol., Columbia Univ., New York.

Mukherjee S 2014 Review of flanking structures in meso- and micro-scales; *Geol. Mag.* **151** 957–974.

Nandy D R 2001 *Geodynamics of northeastern India and the adjoining region*; Rev. edn, Scientific Book Centre, Dispur, Guwahati, Assam, 272p.

Pahari S, Singh H, Prasad I V S V and Singh R R 2008 Petroleum systems of Upper Assam Shelf, India; *Soc. Petrol. Geophysicist, India, Geohorizons*, December 14–21.

Prakash K, Mohanty T, Pati J K *et al.* 2017 Morphotectonics of the Jamini river basin, Bundelkhand craton, Central India, using remote sensing and GIS technique; *Appl. Water Sci.* **7** 3767–3782.

Prasad A S 2014 Flood mitigation through integrated river basin management in lower Brahmaputra river basin, Assam; *Res. Forum: Int. J. Soc. Sci.* **2** 15–22.

Qiao B and Yi C 2017 Reconstruction of Little Ice Age glacier area and equilibrium line attitudes in the central and western Himalaya; *Quart. Int.* **444** 65–75.

Ranga Rao A 1983 Geology and hydrocarbon potential of a part of Assam Arakan Basin and its adjoining region; *Petrol. Asia J.* **VI** 127–158.

Raoof J, Mukhopadhyay S, Koulakov I and Kayal J R 2017 3-D seismic tomography of the lithosphere and its geodynamic implications beneath the northeast India region; *Tectonics* **36** 962–980.

Roy N G and Sinha R 2005 Alluvial geomorphology and confluence dynamics in the Gangetic plains, Farrukhabad-Kannauj area, Uttar Pradesh, India; *Curr. Sci.* **88** 2000–2006.

Sah R K and Das A K 2018 Morphological dynamics of the rivers of Brahmaputra; *J. Geol. Soc. India* **92** 441–448.

Sahoo M and Gogoi K D 2010a Geologic controls on sequence stacking and architecture of Eocene siliciclastic deposits in upper Assam Foreland Basin, India; *Assoc. Petrol. Geol. Bull.* **6** 19–32.

Sahoo M and Gogoi K D 2010b Paleocene to Holocene structure, stratigraphic development and hydrocarbon accumulation in upper Assam foreland basin, India; *Assoc. Petrol. Geol. Bull.* **6** 33–46.

Saikia R R and Amin D N 2016 A study of river channel modifications of Jorhat district of Assam; *Ind. J. History Sci.* **51(3)** 556–559.

Salvany J M 2004 Tilting neotectonics of the Guadiamar drainage basin, SW Spain; *Earth Surf. Process. Landf.* **29** 145–160.

Sarma J N 2005 Fluvial process and morphology of the Brahmaputra river in Assam, India; *Geomorphology* **70** 226–256.

Sarma J N and Phukan M K 2003 Origin and some geomorphological changes of Majuli island of the Brahmaputra river in Assam, India; *Geomorphology* **60** 1–19.

Sarma J N, Shukla A and Gogoi C 2011 Application of DEM, remote sensing and geomorphic studies in identifying a recent [or perhaps Neogene?] Upwarp in the Dibru river basin, Assam, India; *J. Ind. Soc. Remote Sens.* **39** 507–517.

Schumm S A 1956 Evolution of drainage systems and slopes in Badland at Perth Amboy, New Jersey; *Geol. Soc. Am. Bull.* **67** 597–646.

Singh H J, Singh H, Chakrabarti S K, Akhtar M S, Pahari S, Singh R K, Palmowski D and Schenk O 2012 Petroleum system modeling of Assam shelf (northern part) and Naga-Schuppen belt in Assam & Assam Arakan Basin, India; *Assoc. Petrol. Geol. Bull.* **8** 75–81.

Stella J C, Hayden M K, Battles J J, Piegay H, Dufour S and Fremier A K 2011 The role of abandoned channels as refugia for sustaining pioneer riparian forest ecosystems; *Ecosystems* **14** 776–790.

Strahler A 1952 Dynamic basis of geomorphology; *Geol. Soc. Am. Bull.* **63** 923–938.

Talukdar N C, Bhattacharyya D and Hazarika S 2004 Chapter 4: Soil and agriculture; In: *The Brahmaputra basin water resources* (eds) Singh V P, Sharma N and Ojha C S P, Springer, Dordrecht, pp. 35–36, ISBN 978-90-481-6481-3. https://doi.org/10.1007/978-94-017-0540-0.

Toonen W H J, Kleinhans M G and Cohen K M 2012 Sedimentary architecture of abandoned channel fills; *Earth Surf. Process. Landf.* **37** 459–472.

Verhoog F H 1987 Impact of climate change on the morphology of river basins, the influence of climate change and climate variability on the hydrologic regime and water resources; Proceedings of the Vancouver Symposium, August, IAHS Publ. No. 198.315-326.

Verma R K 2002 *Gravity field, seismicity and tectonics of the Indian Peninsula and the Himalayas;* D. Reidel Publishing Company, Dordrecht, 62p, ISBN 978-94-010-8822-0.

Verma R K and Mukhopadhyay M 1977 An analysis of the gravity field in northeastern India; *Tectonophys.* **42** 283–317.

Vita-Finzi C 2012 River history and tectonics; *Phil. Trans. Roy. Soc. A* **370** 2173–2192.

Whitney B B and Hengesh J V 2015 Geomorphological evidence of neotectonic deformation in the Carnarvon basin, Western Australia; *Geomorphology* **228** 579–596.

Whittaker A C 2012 How do landscapes record tectonics and climate?; *Lithosphere* **4** 160–164.

Yadav R and Tiwari V M 2018 Numerical simulation of present day tectonic stress across the Indian subcontinent; *Int. J. Earth Sci.* **107** 2449–2462.

Yin A 2006 Cenozoic tectonic evolution of the Himalayan orogen as constrained by along-strike variation of structural geometry, extrusion history, and foreland sedimentation; *Earth Sci. Rev.* **76** 1–131.

Zámolyi A, Székely B, Draganits E and Timár G 2010 Neotectonic control on river sinuosity at the western margin of the little Hungarian plain; *Geomorphology* **122** 231–243.

Zoback M L 1992 First- and second-order patterns of stress in the lithosphere: The world stress map project; *J. Geophys. Res.* **97** 11703.

Corresponding editor: Saibal Gupta